Radiative Flux from an Argon Plasma

E. A. Brown Jr.* and P. A. Ross†
The Boeing Company, Seattle, Wash.

The radiative flux from argon to the stagnation point of a blunt body was considered. Radiative flux and total heat flux measurements were made in a shock heated argon plasma using a shock tube. The radiation intensity was calculated from the Kramers-Unsöld theory for the continuum, neglecting the line radiation. By taking the lowering of the ionization potential into account in a consistent fashion, the intensity measurements of Petschek et al. and Olsen were shown to be in agreement. The empirical constants, the critical frequency, and effective nuclear charge squared, were estimated to be 1×10^{15} sec^{-1} and 2.7, respectively, from the structure of the argon atom and the intensity measurements. The radiative heat flux measurements agreed with the predictions within the experimental data scatter. The combined radiative and convective heat flux predictions were in agreement with the total heat flux measurements.

Nomenclature

A	=	$(64\pi^{3/2}/36^{1/2})(e^4/m^{3/2}c^3k^{1/2}) = 6.84 \times 10^{-45}$ w-sec-cm^3-°K$^{1/2}$
Z	=	nuclear charge
N_e	=	electron density
T	=	temperature
h	=	Planck's const
R	=	Rydberg const
ν	=	frequency of radiation
n	=	principle quantum number
e	=	electron charge
m	=	electron mass
c	=	speed of light
k	=	Boltzmann const
g_{II}, $\bar{g}_{III}$	=	quantum correction factors $\simeq 1$
I_ν^{ff}	=	intensity per unit volume per unit frequency at ν due to free-free transitions
I_ν^{fb}	=	intensity due to free-bound transitions
T_ν	=	transmission of the window
α_ν	=	absorption of the gage
V	=	volume of radiating gas
r	=	distance from gage to radiating element
θ	=	angle measured from axis of symmetry to the radiating element
$\dot{q}_r$	=	radiant energy per unit area received by gage

I. Introduction

In a gas of sufficiently high temperature, free electrons are present which give rise to energy transport by radiation. If the local radiation intensity is known, the radiative heat flux to the walls may be determined. Herein consideration was given to the relatively simple problem of the radiative flux to the stagnation region of a blunt body in an argon plasma.‡

At relatively low temperatures, the radiation arises from the vibration-rotation band structure associated with the molecules of the gas. At higher temperatures, however, the molecules dissociate and the atoms ionize, giving rise to radiation from the free-free and free-bound electron-ion interactions in addition to the line radiation. Since the dissociation energy is usually lower than the ionization energy, the dissociation process is largely complete at temperatures for which a reasonable amount of ionization is encountered.

In order to study the free-free and free-bound continuum radiation without the complication of the molecular radiation, a noble gas was used. Argon was chosen because of its convenience for shock-tube experiments, the availability of radiation intensity data,[1, 2] and the availability of total heat flux data from this laboratory,[3] as well as from elsewhere.[4]

The continuum radiation from argon requires the presence of free electrons. Consideration of the Saha equation suggests that a reasonable number of free electrons is expected in argon for temperatures above 10,000°K. Since the ionization potential for a number of other gases is not far different from argon, the same should be true. Table 1 indicates the pressure at which 1% and 10% ionization occurs at 10,000°K for several gases and gas mixtures. For a noble gas such as argon, there are two types of radiation: 1) the continuum arising from the free-free and free-bound transitions, and 2) the line radiation arising from the bound-bound transitions. Since the radiant flux and not the details of the spectra were of interest herein, it was assumed that the contribution of the line radiation to the radiative flux was small compared to the continuum radiation. The measurements of Petschek et al.[1] suggest that this assumption was valid.

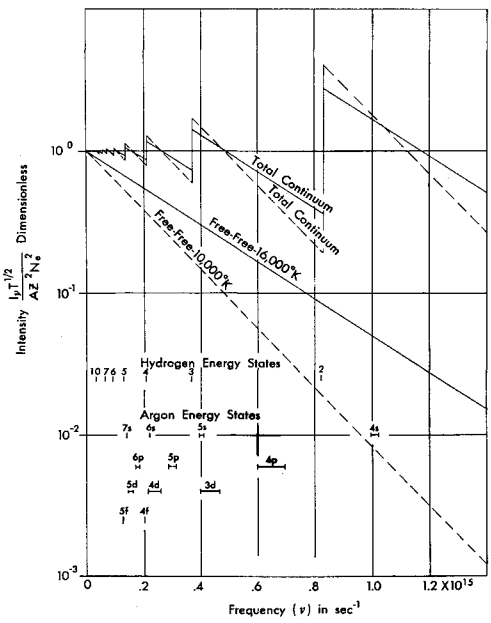

Fig. 1 Continuum radiation for a hydrogen-like gas Z = 1.

Received July 24, 1964; revision received November 30, 1964.

* Staff Member, Flight Sciences Laboratory, Boeing Scientific Research Laboratories. Member AIAA.

† Chief, Combustion-Internal Flow, Turbine Division. Member AIAA.

‡ During the preparation of this manuscript, the recent radiative flux measurements of Rutowski and Bershader[15] came to the attention of the authors.

A blunt-body model with a radiative flux gage was built, and data were obtained in a shock generated argon plasma. These data were compared with the total heat flux measurements made with a model instrumented with a thick film calorimeter gage. The radiation data were compared with the predictions based upon the Kramers-Unsöld theory for the continuum radiation. In the next section, a discussion of the Kramers-Unsöld radiation theory and the extent to which it applies to argon is given. The third section gives a description of the radiation flux gage and the shock-tube experiments. The fourth section compares the radiative flux data with the predictions, and compares the radiative and total flux measurements.

II. Theoretical Radiation Intensity

In order to determine the radiative flux, it is necessary to know the radiation intensity of the gas and its spectral characteristics. A radiation intensity theory for argon has not been calculated; however, a reasonable estimate may be made from the calculations for the hydrogen-like atom.

A number of authors have contributed to the calculation of the continuum radiation from hydrogen-like atoms. Kramers[5] gave a classical treatment of the problem in 1923, which was extended by Unsöld[6] to hydrogen-like atoms. A quantum mechanical treatment of the free-free and free-bound transitions of hydrogen-like atoms was given by Menzel and Pekeris.[7] A good review of the hydrogen-like atom calculations was given by Pomerantz.[8]

The calculation of the intensity per unit volume for unit frequency based upon hydrogen wave functions results in

$$I_\nu^{ff} = (AZ^2N_e^2/T^{1/2})\,\bar{g}_{III}e^{-h\nu/kT} \tag{1}$$

$$I_\nu^{fb} = A\,\frac{Z^2N_e^2}{T^{1/2}}\,\frac{2hRZ^2}{kT}\,e^{-h\nu/kT}\sum_{n=n_0}^{\infty}\frac{g_{II}}{n^3}\,e^{hRZ^2/n^2kT}$$

$$n_0 \geq \left(\frac{RZ^2}{\nu}\right)^{1/2} \tag{2}$$

In the region where the bound energy states are sufficiently dense, the sum in Eq. (2) may be approximated by an integral. Let n_c be the minimum principle quantum number for which the states are dense; then,

$$I_\nu^{fb} = \frac{AZ^2N_e^2}{T^{1/2}}\,e^{-h\nu/kT}\left[\frac{2hRZ^2}{kT}\left(\sum_{n_0}^{n_c-1}\frac{g_{II}}{n^3}\exp(hRZ^2/n^2kT) + \bar{g}_{II}\exp(h\nu^*/kT) - 1\right)\right] \tag{3}$$

where

$$\nu^* = \begin{cases}\nu \text{ for } \nu \leq \nu_c\\ \nu_c \text{ for } \nu > \nu_c\end{cases}$$

$$\nu_c = RZ^2/n_c^2$$

$$\bar{g}_{II} = \text{mean value of } g_{II} \simeq 1$$

Equations (1) and (3) may be combined to give the total continuum radiation as follows wherein $\bar{g}_{III} \simeq \bar{g}_{II} \simeq 1.0$:

$$I_\nu = AZ^2N_e^2/T^{1/2} \qquad \nu \leq \nu_c \tag{4}$$

$$I_\nu = \frac{AZ^2N_e^2}{T^{1/2}}\left[\exp - [h(\nu-\nu_c)/kT] + \frac{2hRZ^2}{kT}\sum_{n_0}^{n_c-1}\frac{\exp - \{h[\nu - (RZ^2/n^2)]/kT\}}{n^3}\right] \qquad \nu > \nu_c \tag{5}$$

A plot of I_ν is given in Fig. 1 from Eqs. (4) and (5) for $Z^2 = 1$, $n_c = 10$, and $T = 10{,}000°$ and 16,000°K. From this it is clear that no significant error is involved for $n_c = 6$, and the error only becomes appreciable for $n_c < 4$.

Table 1 Pressure for 1% and 10% ionization at 10,000°K

	1%	10%
He	10^{-1} atm	...
Ne	10^{-3}	10^{-5}
A	10	10^{-3}
Kr	10	10^{-2}
H_2	10	10^{-1}
Air	10	10^{-2}
50% CO_2, 25% N_2, 25% A	10	10^{-2}

Argon, however, is not a hydrogen-like atom. The ground state of the argon atom has the $3s$ and $3p$ states filled; and the ground state of the ion has one of the $3p$ electrons removed. Thus, argon may be considered a nucleus composed of the ground state ion ($3s^23p^5$) with a nuclear charge ($Z = 1$), and a single electron. To this extent argon may be considered hydrogen-like. This approximation may be checked by determining the effective nuclear charge for the various excited states of the atom. Table 2 shows the Z^2 values for the principle quantum numbers up to 10 and the angular momentum quantum numbers up to 3 from the data of Moore.[9] The s and p states are not properly represented by the hydrogen model; however, for $n \geq 6$ the s and p states represent 10% or less of the states associated with a principle quantum number. Therefore, the argon intensity should be represented by Eq. (4) with $Z = 1$ up to a frequency of 1×10^{14} sec^{-1}.

For the higher frequencies, the major contribution to the intensity is due to free-bound transitions into states with small principle quantum numbers. Also indicated in Fig. 1 are the frequencies corresponding to s, p, d, and f states for the smaller principle quantum numbers. This indicates that the states were sufficiently dense out to the $4s$ state so that it is reasonable to replace the sum by an integral out to a frequency of 1×10^{15} sec^{-1}. This region of the spectrum is dominated by the states for which $Z^2 > 1$. Therefore, the intensity averaged over a reasonable frequency may be represented by Eq. (4) for 1×10^{14} sec$^{-1} \leq \nu \leq 10 \times 10^{15}$ sec^{-1} with $Z_{\text{eff}}^2 > 1$, i.e., $\nu_c = 1 \times 10^{15}$ sec^{-1}. The foregoing representation is, of course, not correct in detail. For radiative heat transfer considerations wherein the spectral average is sufficient, this representation is satisfactory.

Table 2 indicates that the maximum value for Z^2 is 5 for the $4s$ state; therefore, the Z_{eff}^2 value to be used in Eq. (4) should be between 1 and 5. Petschek et al.[1] have made intensity measurements at three frequencies (0.42, 0.60, and 0.71×10^{15} sec^{-1}) in the temperature-density range of interest. This data showed reasonable agreement with Eq.

Table 2 Z^2 for argon

n	s	p	d	f
10	1.62	1.41	1.03	1.00
		1.45	1.10	
9	1.72	1.46	1.03	1.00
		1.52	1.11	
8	1.86	1.56	1.06	1.00
		1.63	1.15	
7	2.07	1.66	1.07	1.00
		1.75	1.15	
6	2.40	1.85	1.06	1.00
	2.43	1.97	1.19	
5	3.06	2.17	1.07	1.00
	3.11	2.38	1.21	
4	4.82	2.88	1.09	1.00
	4.93	3.36	1.25	
3	...	...	1.09	...
	...	...	1.26	...

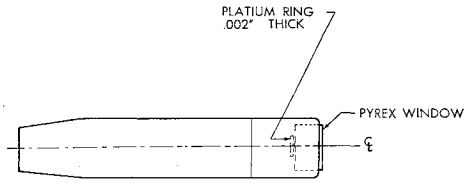

Fig. 2 Sketch of radiation heat flux gage.

(4) with $Z_{\text{eff}}^2 = 2.7$. Olsen[2] has made intensity measurements from an argon arc at 16,000°K and 1 atm. An approximate integration of the intensity over the frequency range of 0.2×10^{15} sec^{-1} to 1×10^{11} sec^{-1} results in an average value of $Z_{\text{eff}}^2 = 2.2$. At the frequencies of Petschek's measurements, Olsen's data results in $Z_{\text{eff}}^2 \simeq 2$.

It should be noted that the data of Petschek et al. and Olsen are not directly comparable because of the manner in which the data were compared with theory. In the case of Olsen's data, the plasma temperature was measured by observing the argon line intensity, and the electron density was calculated from the measured temperature and pressure. The data of Petschek et al. were obtained in a shock tube where the electron density and temperature were calculated from the measured shock Mach number and the initial shock tube pressure. That is, the measurement of the shock Mach number measures the energy of the plasma rather than the temperature. Since the basic measurements were different for the two sets of data, the accuracy of the thermodynamic calculations will influence the predicted electron density (and the temperature for the shock-tube case), and thus the predicted intensity.

The most important influence on the thermodynamic calculations was the consideration of the interaction energy due to the presence of charged particles. The effects of the long range interaction of the charged particles may be taken into account in an approximate manner by reducing the ionization potential in the Saha equation. In determining the Z_{eff}^2 from the shock-tube data of Petschek et al., no such correction was made, whereas, the Z_{eff}^2 from Olsen's arc data does include a correction for the lowering of the ionization potential. In order to determine the Z_{eff}^2 from the shock-tube data including the effect of the interaction energy requires that the normal shock and thermodynamic calculations be carried out with the corrected ionization potential.

Pomerantz[8] has carried out these calculations with and without the corrected ionization potential using Ecker and Weizel's[10] formula for the lowering of the ionization potential.

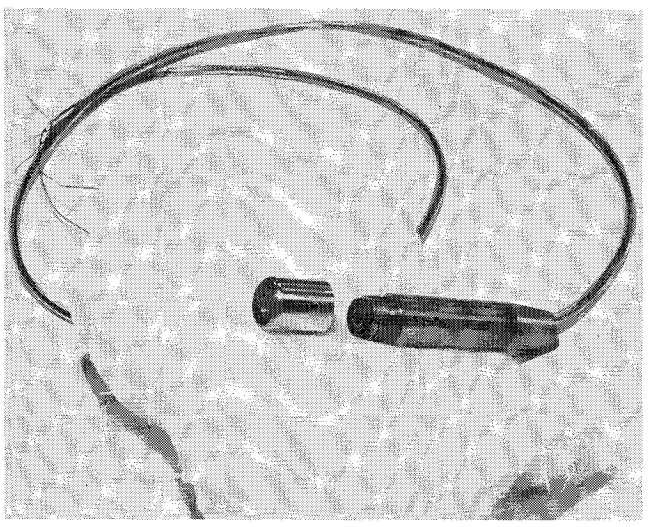

Fig. 3 Radiation heat flux gage assembly.

When the lowering of the ionization potential was taken into account, there was a reduction in the temperature and an increase in the electron density at a given shock Mach number. The comparison of the predicted intensity for the shock-tube conditions of $P_1 = 10$ mm Hg and shock Mach number of 10–15 indicates that the inclusion of the corrected ionization potential reduces the value of Z_{eff}^2 about 20%. If the corrected ionization potential were taken into account without correcting the temperature as suggested by Petschek et al., Z_{eff}^2 would be reduced by a factor of 2 or more. Based upon the foregoing considerations, the Z_{eff}^2 from the measurements of Petschek et al. may be put on a comparable basis with the measurements of Olsen. This results in $Z_{\text{eff}}^2 = 2.1$ for the shock-tube data as compared with $Z_{\text{eff}}^2 = 2$ for the arc data in the same frequency range.

From the foregoing theoretical considerations and comparison with experimental intensity data, a reasonable representation of the mean intensity is

$$I_\nu \begin{cases} = AZ_{\text{eff}}^2 (N_e^2/T^{1/2}) & \nu < 1 \times 10^{15} \text{ sec}^{-1} \\ = 0 & \nu > 1 \times 10^{15} \text{ sec}^{-1} \end{cases} \quad (6)$$

Olsen's data suggests that the decrease in intensity with frequency was much sharper than predicted by Eq. (5); therefore, the intensity contribution for frequencies above 1×10^{15} sec^{-1} was neglected. The reduction in the critical frequency due to the lowering of the ionization potential caused by the long range forces and the bound-bound continuum radiation from the smeared, densely packed bound states has been neglected. The contribution of free-bound transitions to the ground state has also been neglected. The discussion in Sec. IV indicates that for the conditions of interest, this region of the spectrum was strongly self-absorbing and may be neglected.

The appropriate value of Z_{eff}^2 to be used depends upon the manner in which the thermodynamic state is determined. The foregoing considerations would indicate that $Z_{\text{eff}}^2 \simeq 2$ is reasonable if the thermodynamic state, i.e., N_e and T, are determined with due consideration of the reduced ionization potential. As discussed by Olsen,[2] the magnitude of the correction to the ionization potential is still in question; therefore, the determination of Z_{eff}^2 from the measured intensity data is also subject to question. For the shock-tube measurements considered herein, the normal shock and thermodynamic properties were calculated without correcting the ionization potential; therefore, Z_{eff}^2 will be taken to be 2.7.

III. Experimental Data

Two types of heat flux measurements were reported herein: radiative flux and total heat flux. A 1-in. cold gas driven shock tube with argon as the test gas was used for the experiments. The shock tube consisted of a $3\frac{1}{2}$-in.-i.d. driver, a $3\frac{1}{2}$-in.-i.d. buffer and a 1-in.-i.d. driven section. Cold helium was used as the driver and buffer gas. A more detailed description of the shock tube and its performance has been reported elsewhere.[11] All of the data reported herein were obtained with the driven section initial pressure (P_1) at 10 mm Hg. The total heat flux data were obtained over the shock Mach number range of 4.5 to 12, whereas the radiative flux data covered a Mach number range of 10 to 12.5.

The total heat flux measurements were made on a hemisphere-cylinder model. The heat flux gage was a thick film calorimeter type using resistance thermometry to measure the temperature. The gage consisted of 0.002-in.-thick platinum foil flush mounted on pyrex. A more detailed description of the gage and its calibration were reported elsewhere.[12]

The radiative flux measurements utilized a gage of the thick film calorimeter type similar to that used for the total flux measurements. The gage element was located inside the body and isolated from the flow by a pyrex window (see

Figs. 2 and 3). In order to obtain a reasonable viewing angle, the nose was flat rather than hemispherical as in the case of the total flux measurements. In order to avoid deterioration of the transmission characteristics of the pyrex window, it was changed after each run. The minimum signal measurable by the gage was approximately 0.03 kw/cm^2, which limited the minimum shock Mach number to 10 at 10 mm Hg initial pressure for which radiative flux data could be obtained.

In addition to the heat flux measurements, direct emission photographs of the flow were obtained. An Abtronic image converter camera with an effective exposure time of 10^{-7} sec was used. A series of photographs of the flow about the blunt body used for the radiative flux measurements is shown in Fig. 4. These show the flow development as a function of time after the incident shock arrived at the model. These measurements, in conjunction with the heat flux traces (see Fig. 5), indicated that the flow was well developed and the radiative flux constant from 15 μsec to about 50 μsec after the arrival of the incident shock. In addition to the information on the flow development and breakdown obtained from the photographs, the shock standoff distance was measured.

The accuracy of the total heat flux data was $\pm 15\%$ and the radiative data was $\pm 30\%$. These accuracy figures include the heat flux gage calibration, the initial pressure gage calibration, the accuracy of the shock Mach number timing corrected for shock attenuation, and the reading errors associated with the heat flux traces. The lower accuracy of the radiation flux data was largely attributed to the lower signal to noise ratio for the heat flux data at the same shock Mach numbers.

IV. Discussion

In order to relate the radiation intensity to the heat flux measurements, due consideration must be given to the gage geometry, the effective volume of the radiating gas, and the amount of incident radiation absorbed by the gage. A detailed account of these considerations is given below for the flat-nosed body used for the radiative flux measurements.

Assuming that the shock layer may be represented as an infinite slab, and neglecting absorption and stimulated emission in the shock layer, the heat flux to the gage was given by

$$\dot{q}_r = \int_V \int_0^\infty \frac{I_\nu T_\nu \alpha_\nu d\nu}{4\pi r^2} \cos\theta \, dV \tag{7}$$

The geometry for the shock layer and gage is shown in Fig. 6.

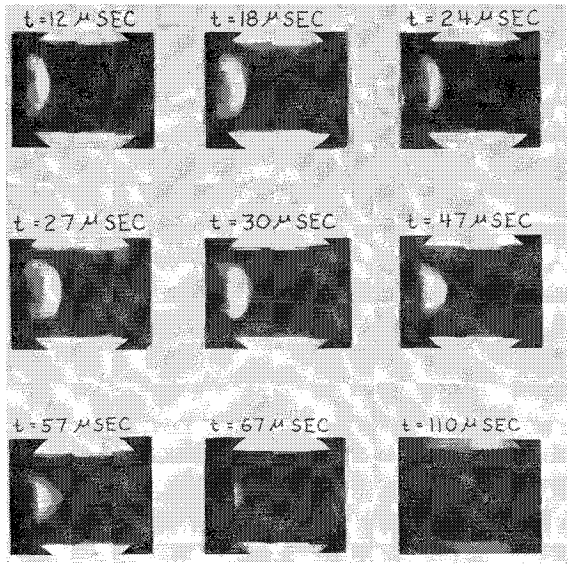

Fig. 4 Flow development over a blunt body in argon.

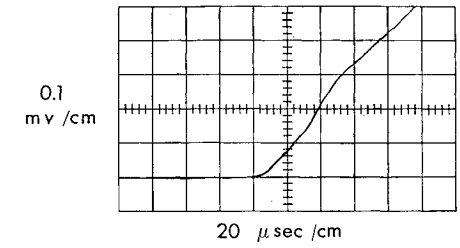

Fig. 5 Sample oscillogram of radiation heat flux gage output.

Since the shock layer is thin compared to the body radius of curvature, the assumption that the shock layer may be represented by an infinite slab was valid. In order to determine the validity of neglecting absorption and stimulated emission, the optical depth was introduced:

$$\tau_\nu \equiv \int_0^x \frac{I_\nu}{4\pi B_\nu} dx \tag{8}$$

where τ_ν = optical depth, and $B_\nu = 2h\nu^3/c^2(e^{h\nu/kT} - 1)$.

As long as the optical depth is small compared to one, absorption may be neglected. On the other hand, however, if the optical depth is large compared to one, the radiation is strongly absorbed and the surface of such a radiating gas acts like a black body.

In order to proceed further, it is necessary to consider the specific characteristics of the radiating source and the gage. Using Eq. (6) for I_ν, the optical depth based upon the shock standoff distance may be calculated.

$$\tau_\nu(\delta) = (I_\nu/4\pi B_\nu)\delta \tag{9}$$

The measured shock standoff distance was 5 ± 1 mm. The maximum intensity was encountered at the maximum shock Mach number 12. The optical depth for these conditions was calculated for three frequencies: ν_c, 0.1 ν_c, and the band edge for transition to the ground state ν_{gs}. They are shown in Table 3.

The calculation shown in Table 3 for the optical depth indicates that no serious absorption was encountered in the frequency range 0.1×10^{15} to 1×10^{15} sec^{-1}, and that any radiation arising from transitions to the ground state at the same intensity as that at the lower frequency would be strongly self-absorbed and thus may be neglected.

The transmission characteristics of the pyrex window were obtained from the manufacturer, and the absorption of the gage element was obtained from the reflection coefficient of polished platinum. A plot of T_ν, α_ν, and their product is shown in Fig. 7. This indicates that the band pass of the gage is within the frequency range for which self-absorption may be neglected.

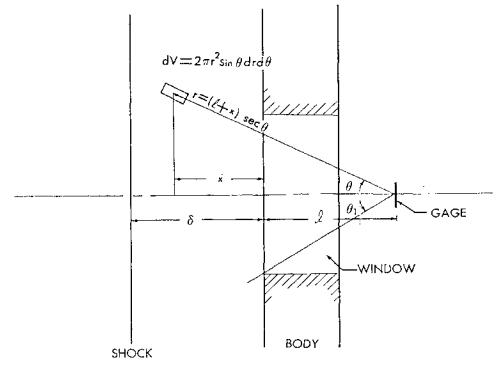

Fig. 6 Sketch of shock layer geometry.

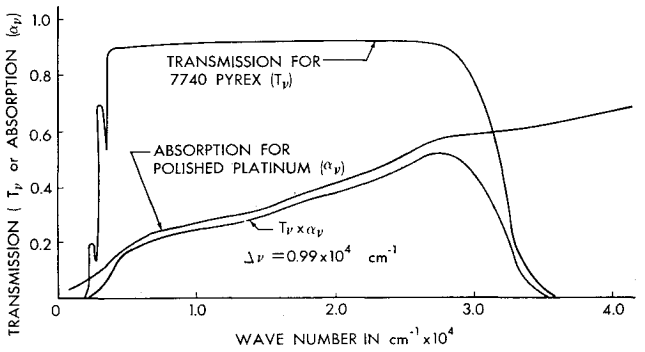

Fig. 7 Transmission for pyrex and absorption for platinum as a function of wave number.

Making use of the foregoing information, Eq. (7) may be integrated to give the energy received by the gage:

$$\dot{q} = \frac{I_\nu \Delta_\nu}{2}(1 - \cos\theta_1)\delta \qquad \Delta_\nu = \int_0^\infty T_\nu \alpha_\nu d\nu \qquad (10)$$

The measured radiative flux was compared with the flux as calculated by Eq. (10). The calculated flux was based upon the measured shock standoff distance, the gage characteristics determined as described previously, and the intensity as given by Eq. (6). The electron density and temperature in the shock-layer region were obtained from the calculations of Arave et al.[13] Since this calculation neglects the lowering of the ionization potential, Z_{eff}^2 was taken to be 2.7. The measured and calculated radiative flux is plotted vs shock Mach number on Fig. 8. The agreement between the calculated and measured values was well within the scatter of the experimental data.

It should be noted that only about 5% of the total radiative flux incident on the body was measured by the radiation gage because of the limited viewing angle and limited spectral response. Approximately 10% of the total energy was excluded because of the cutoff of the pyrex window on the low frequency end of the spectrum and 5% on the high frequency

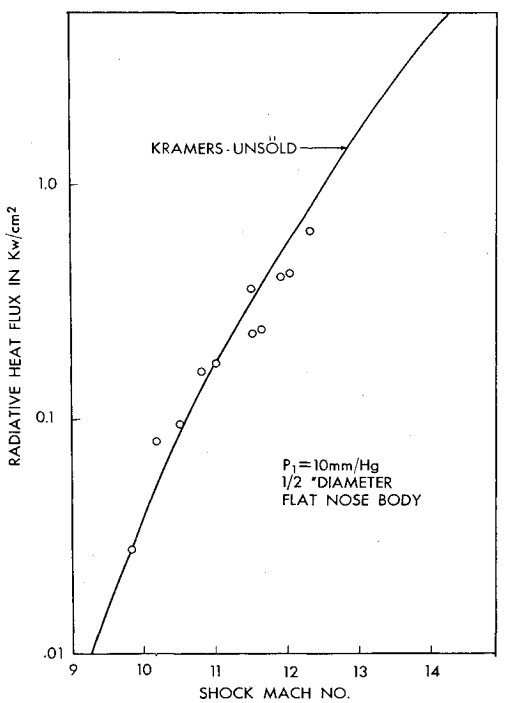

Fig. 8 Radiative heat flux to the stagnation point of a blunt body in argon.

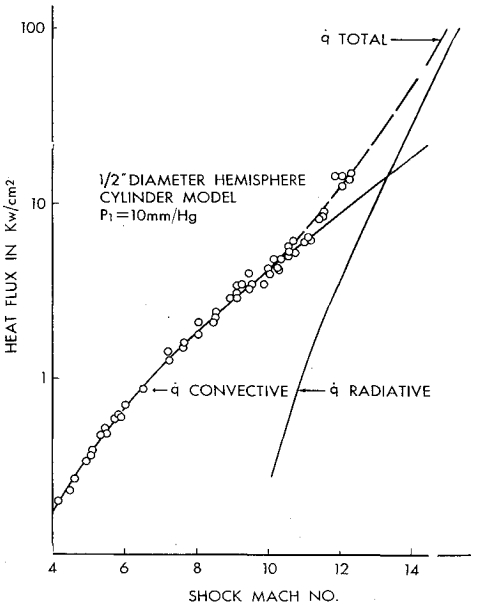

Fig. 9 Heat transfer to the stagnation point of a blunt body in argon.

end. The major reduction of the incident flux was due to the limited viewing angle and to a lesser extent the absorption coefficient of the platinum.

Heat flux measurements with an exposed heat flux gage have also been measured. This data is shown in Fig. 9.[3] Similar measurements have been made by Rutowski and Bershader[4] which were essentially in agreement with those shown in Fig. 9. The transport properties of argon, including charge exchange, used in the numerical integration of the boundary-layer equations were obtained from Pindroh.[14] The convective heat flux based upon these calculations is shown in Fig. 9. Also shown in Fig. 9 is the radiative flux contribution calculated in a manner similar to that previously outlined with due consideration for the increased view angle, the reduced standoff distance of the spherical nose, and the increased spectral response in the absence of the window. Although the radiative contribution was less than the convective contribution at the maximum shock Mach number, it was nevertheless substantial, and in agreement with the predicted total heat flux. To the extent that no substantial increase in the radiative flux in excess of that accounted for by Eq. (6) is evident by the data shown in Fig. 9, there is no large contribution to the radiative flux at frequencies above 1×10^{15} sec^{-1}.

It should be noted that care must be exercised in extending the radiative flux predictions beyond a shock Mach number of 12 without consideration of self-absorption. For example, the optical depth increases approximately a factor of 4 at the shock Mach number of 13 due to the large increase in electron density.

V. Conclusions

It may be concluded that a reasonable understanding of radiative heat flux from ionized argon was obtained. The quantitative prediction of the heat flux, however, is based upon a semi-empirical theory. A qualitative argument was used to determine the spectral region that contributes to the continuum radiative flux, and the value of the effective nuclear charge squared was only determined within a factor of 5. The final values of ν_c and Z_{eff}^2 used for the heat flux calculations were based upon measured intensity data. The assumption of neglecting the line radiation was justified on the basis of the measured heat flux. The present calculations

Table 3 Shock-layer optical depth

ν	$\tau_\nu(\delta)$
ν_c	0.0225
$0.1\ \nu_c$	0.289
ν_{gs}	13.1[a]

[a] The low frequency value of I_ν was used.

make no attempt to explain the detailed spectral characteristics of the radiation.

The question of the interrelationship of the effective nuclear charge and the lowering of the ionization potential was circumvented by utilizing empirical data. Consistent consideration of the lowering of the ionization potential brought the measured value of the nuclear charge obtained by Petschek et al. and Olsen into agreement.

Much remains to be investigated both experimentally and theoretically in order to understand the detailed spectral characteristics. Such information would be required if self-absorption has to be taken into account and/or if the absorption characteristics of the body receiving the radiation has large variations with frequency. A more careful consideration of the transitions to the ground state may well be important for conditions other than the ones considered in these tests. The question of the importance of the line radiation has only been considered in a gross sense. The extension to other gases, even noble gases, require at least enough intensity data to establish the critical frequency and the effective nuclear charge.

References

[1] Petschek, H. E., Rose, P. H., Glicke, H. S., Kane, A., and Kantrowitz, A., "Spectroscopic studies of highly ionized argon produced by shock waves," J. Appl. Phys. **26**, 83–95 (1955).

[2] Olsen, H. N., "Partition function cutoff and lowering of the ionization potential in an argon plasma," Phys. Rev. **124**, 1703–1708 (1961).

[3] Ross, P. A., "Shock tube data report on stagnation point heat transfer in argon," The Boeing Company, Doc. D2-22007 (1963).

[4] Bershader, D. and Rutowski, R. W., "Studies of an argon shock-layer plasma," *Magnetohydrodynamics, Proceedings of the Fourth Biennial Gas Dynamics Symposium*, edited by A. B. Cambel, T. P. Anderson, and M. M. Slawsky (Northwestern University Press, Evanston, Ill., 1962), pp. 129–140.

[5] Kramers, H. A., "On the theory of x-ray absorption and of the continuous x-ray spectrum," Phil. Mag. **46**, 836–871 (1923).

[6] Unsöld, A., "Uber das Kontinuierlicke Spectrum der Hg-Hochdrucklampe, des Unterwasserfunkens und ähnlicker Gasentladungen," Ann. Physik **33**, 607–616 (1938).

[7] Menzel, D. H. and Pekeris, C. L., "Absorption coefficients and hydrogen line intensities," Monthly Notices Royal Astron. Soc. **96**, 77–111 (1935).

[8] Pomerantz, J., "The influence of the absorption of radiation in shock tube phenomena," J. Quant. Spectry. Radiative Transfer **1**, 185–248 (1961).

[9] Moore, C. E., "Atomic energy levels," National Bureau of Standards Circ. 467, Vol. 1, pp. 211–218. (1949).

[10] Ecker, G. and Weizel, W., "Zustandssumme und effektive Ionisierungsspannung eines Atomis im Inneren Plasmas," Ann. Physik **17**, 126–140 (1956).

[11] McDill, P. L., Brown, E. A., Ross, P. A. and Huseby, O. A., "The performance of a buffered shock tube with area reduction," *Advances in Hypervelocity Techniques, Proceedings of the Second Symposium on Hypervelocity Techniques*, edited by A. M. Krill (Plenum Press, New York, 1962), pp. 749–772.

[12] Ross, P. A. and Brown, E. A., "An assessment of errors involved in thick-film heat transfer measurements," The Boeing Company, Doc. D2-22006 (1962).

[13] Arave, R. J. and Huseby, O. A., "Aerothermodynamic properties of high temperature argon," The Boeing Co., Doc. D2-11238 (1962).

[14] Pindroh, A. L., "Charge exchange effects on transport properties," Phys. Fluids (to be published).

[15] Rutowski, R. W. and Bershader, D., "Shock tube studies of radiative transport in an argon plasma," Phys. Fluids **7**, 568–577 (1964).